Electronic Interactions in Aryne Biradicals. Ab Initio Calculations of the Structures, Thermochemical Properties, and Singlet−Triplet Splittings of the Didehydronaphthalenes

Robert R. Squires[§,†] and Christopher J. Cramer*[,‡]

Department of Chemistry, Purdue University, West Lafayette, Indiana 47907, and Department of Chemistry and Supercomputer Institute, University of Minnesota, Minneapolis, Minnesota 55455-0431

Received: August 21, 1998

Structural and energetic properties for the lowest energy singlet and triplet states of the 10 didehydronaphthalene isomers are predicted using density functional and multireference second-order perturbation theories. These levels of theory offer excellent agreement with known heats of formation for three singlet isomers when appropriate isodesmic equations are used for prediction. Singlet−triplet splittings and biradical stabilization energies are examined to gain insight into the degree of interaction between the biradical centers. This interaction operates via three distinct mechanisms, namely, through space (overlap), through σ-bonds, and through π-bonds, in order of increasing distance over which quantitative impact is predicted. The first two effects are especially sensitive to the relative orientations of the biradical centers and the shape of the molecular framework that joins them. Simpler models are examined for their utility in predicting singlet−triplet splittings; proton hyperfine splittings in antecedent monoradicals are the best predictors of biradical-state energy splittings.

Introduction

Drug design is motivating new developments in biradical chemistry. The discovery that *p*-benzyne-,[1,2] didehydroindene,[3,4] and α,3-dehydrotoluene-type[5,6] biradicals participate in the DNA-cleaving activity of enediyne and related antibiotics has inspired numerous investigations aimed at understanding the nature of these biradical intermediates and optimizing their in vivo activity.[7] Two important goals of this research are characterizing the chemical triggering mechanisms that promote biradical formation through Bergman cyclization[8,9] and its variants[10−19] and controlling the reactivity and, therefore, selectivity of the biradical intermediates in the hydrogen atom abstraction processes that are believed to initiate DNA cleavage.[20] Chen and co-workers have advanced a simple model for this latter problem which correlates the reactivity of singlet-state biradicals with the magnitude of their singlet−triplet (S−T) energy splittings, ΔE_{ST}; the larger the splitting for a singlet ground state, the greater the barrier for H-atom abstraction and, hence, the more selective the biradical.[21−23] Therefore, understanding what controls the magnitude of S−T splittings in biradicals can facilitate the rational design of more selective DNA-cleaving agents.

Didehydroarenes ("arynes"), including the benzyne archetypes and their heteroaromatic homologues, are especially useful paradigms for investigating the relationships between structure, reactivity, and S−T splitting in (σ,σ) biradicals, i.e., biradicals in which the two formally nonbonding electrons occupy two relatively localized, in-plane σ orbitals. The rigid molecular framework of these compounds and the well-defined distance and relative orientation of the radical lobes at the two dehydro centers provide an ideal situation for systematic investigations of through-bond and through-space electronic interactions. In their seminal theoretical paper on through-bond coupling, Hoffmann, Imamura, and Hehre[24] (HIH) employed extended Hückel calculations on a series of didehydroaromatic molecules (including benzynes, didehydronaphthalenes, -acenaphthenes, -azulenes, and others) in order to look for patterns in the valence orbital splittings and to identify the basic coupling unit between the two σ radical sites. They concluded that the magnitude of the coupling depended upon both the relative orientation of the radical lobes and the number and orientation of the intervening σ-bonds. HIH also concluded that for through-bond interactions over an odd number of σ-bonds (greater than 1) the antisymmetric combination of the two radical orbitals will generally be lower in energy than the symmetric combination because of the availability of suitably aligned, unfilled σ^* orbitals that contribute to the hybrid biradical MO. For instance *p*-benzyne, a 1,4-biradical with little direct overlap between the biradical orbitals, has two identical 3-bond coupling paths that are suitably aligned to make the antisymmetric combination orbital Ψ^- fall

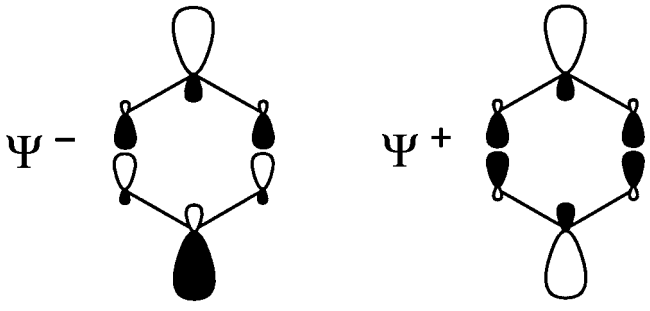

well below the symmetric combination orbital Ψ^+. In principle, the extent of through-bond coupling in a series of arynes should be related to their S−T splittings and their relative stabilities.[25−27] While this relationship has been thoroughly examined for *o*-, *m*-, and *p*-benzyne[28] and the six isomeric pyridynes,[29] its broader scope for larger systems has not been explored.

In this paper we present a detailed theoretical examination of the geometries, electronic interactions, and energetics of the

† Purdue University.
‡ University of Minnesota.
§ Deceased.

10.1021/jp983449b CCC: $15.00
Published on Web 10/16/1998

TABLE 1: Point Group Symmetries and Active Spaces for Didehydronaphthalenes, Benzynes, and Ancillary Hydrocarbons

			active space	
molecule	point group	electronic state	no. of electrons	orbitals
acetylene	D_{2h}[a]	^1A_g	4	$1b_{2g}$, $1b_{2u}$, $1b_{3g}$, $1b_{3u}$
ethylene	D_{2h}	^1A_g	2	$1b_{2g}$, $1b_{3u}$
o-benzyne	C_{2v}	$^1A_1$, $^3B_2$	8	$10a_1$, $1-3a_2$, $1-3b_1$, $8b_2$
m-benzyne	C_{2v}	^1A, $^3B_2$	8	$11a_1$, $1-2a_2$, $1-4b_1$, $7b_2$
p-benzyne	D_{2h}	^1A_g, $^3B_{1u}$	8	$6a_g$, $1a_u$, $1b_{1g}$, $5b_{1u}$, $1-2b_{2g}$, $1-2b_{3u}$
phenyl radical	C_{2v}	$^2A_1$	7	$11a_1$, $1-2a_2$, $1-4b_1$
benzene	D_{2h}[a]	^1A_g	6	$1a_u$, $1b_{1g}$, $1-2b_{2g}$, $1-2b_{3u}$
1,2-didehydronaphthalene	C_s	$^1A'$, $^3A'$	12	$28-29a'$, $1-10a''$
1,3-didehydronaphthalene	C_s	$^1A'$, $^3A'$	12	$28-29a'$, $1-10a''$
1,4-didehydronaphthalene	C_{2v}	$^1A_1$, $^3B_2$	12	$16a_1$, $1-5a_2$, $1-5b_1$, $13b_2$
1,5-didehydronaphthalene	C_{2h}	^1A_g, ^3B_u	12	$15a_g$, $1-5a_u$, $1-5b_g$, $14b_u$
1,6-didehydronaphthalene	C_s	$^1A'$, $^3A'$	12	$28-29a'$, $1-10a''$
1,7-didehydronaphthalene	C_s	$^1A'$, $^3A'$	12	$28-29a'$, $1-10a''$
1,8-didehydronaphthalene	C_{2v}	$^1A_1$, $^3B_2$	12	$16a_1$, $1-5a_2$, $1-5b_1$, $13b_2$
2,3-didehydronaphthalene	C_{2v}	$^1A_1$, $^3B_2$	12	$16a_1$, $1-5a_2$, $1-5b_1$, $13b_2$
2,6-didehydronaphthalene	C_{2h}	^1A_g, ^3B_u	12	$15a_g$, $1-5a_u$, $1-5b_g$, $14b_u$
2,7-didehydronaphthalene	C_{2v}	$^1A_1$, $^3B_2$	12	$16a_1$, $1-5a_2$, $1-5b_1$, $13b_2$
1-naphthyl radical	C_s	$^2A'$	11	$29a'$, $1-10a''$
2-naphthyl radical	C_s	$^2A'$	11	$29a'$, $1-10a''$
naphthalene	D_{2h}	^1A_g	10	$1\text{-}2a_u$, $1-2b_{1g}$, $1-3b_{2g}$, $1-3b_{3u}$

[a] Highest available symmetry in MOLCAS 3.0.

ten isomeric didehydronaphthalenes ("naphthalynes"). The naphthalynes have a long history of experimental investigation, and they are the subjects of renewed interest for their potential role in drug design. As in classical benzyne synthesis, 1,2- and 2,3-naphthalynes can be generated by base-induced elimination reactions of halonaphthalenes.[30,31] Didehydronaphthalenes (DDN's) have also been generated in solution by thermal rearrangements of substituted 1,5-didehydro[10]annulenes,[32] 1,6-didehydro[10]annulene,[33] and *o*-dialkynylbenzenes,[13,34-37] by tandem Bergman cyclization of (*Z*,*Z*)-deca-3,7-diene-1,5,9-triyne,[38] and by oxidation of aminotriazines.[39] They have also been formed in a low-temperature matrix by pyrolysis of 2,3-naphthalene anhydride[40] and in the gas phase by dissociative electron ionization[41,42] and anion-induced elimination reactions.[43] Previous theoretical investigations of the DDN's are limited to the extended Hückel study by HIH[24] and some semiempirical calculations on 1,2- and 2,3-naphthalyne reported by Ford and Biel.[44]

In the present work we employ ab initio methods, including multireference second-order perturbation theory (CASPT2) and density functional theory (DFT), to derive thermochemical properties and S−T splittings for all ten naphthalynes. We recently applied these same computational methods, as well as coupled-cluster methods, in a theoretical study of the structures, thermochemistry, and S−T splittings of the benzynes[45,46] and pyridynes.[29,46] In one of these studies[45] we were able to correct errors in the literature[47] concerning the predicted thermochemistry of singlet benzynes and the energetics of the Bergman cyclization obtained from CASPT2 calculations. We were also able to show that coupled-cluster calculations that include effects due to triple excitations (i.e., CCSD(T)) perform remarkably well in predicting the experimentally determined thermochemistry[48-50] and S−T splittings[51] of the benzynes. The performance of DFT calculations was also evaluated and found to be less uniformly reliable, particularly with respect to energetics, due to the limitations of a single-configuration representation of the benzyne singlets with relatively high biradical character, i.e., *p*-benzyne and, to a lesser extent, *m*-benzyne. In a preliminary account of our naphthalyne results,[52] we demonstrated a linear relationship between S−T splittings of naphthalynes as obtained from CASPT2 calculations, and ^{1}H hyperfine coupling constants in corresponding naphthyl monoradicals as obtained from DFT calculations. The relationship was used, together with scale factors derived from comparing the CASPT2 splittings to experimental values for the benzynes, to derive new predictions for the S−T splittings of all ten naphthalyne biradicals. Here we elaborate on the electronic structures of the various naphthalyne biradicals with the expectation that aspects of this analysis will be *generally* applicable to large aromatic (σ,σ) biradicals.

Computational Methods

Molecular geometries for all species were optimized at the multiconfiguration self-consistent-field (MCSCF) and DFT levels of theory using the correlation-consistent polarized valence-double-ζ (cc-pVDZ[53]) basis set. The MCSCF calculations were of the complete active space (CAS) variety and are described further below. The DFT calculations employed the gradient corrected functionals of Becke[54] for exchange energy and Perdew et al.[55] for correlation energy (BPW91). All DFT geometries were confirmed as local minima by computation of analytic vibrational frequencies, and these frequencies were used to compute zero-point vibrational energies (ZPVE) and 298 K thermal contributions ($H_{298} - E_0$) for all species. DFT calculations on doublet and triplet spin states employed an unrestricted formalism. Total spin expectation values for Slater determinants formed from the optimized Kohn−Sham orbitals did not exceed 0.77 and 2.02 for doublets and triplets, respectively.

To improve the molecular orbital calculations, dynamic electron correlation was accounted for by using multireference second-order perturbation theory (CASPT2) for the CAS reference wave functions; these calculations were carried out for the CAS optimized geometries. In general, then, our electronic energies are of the CASPT2/cc-pVDZ//CAS/cc-pVDZ variety, and we derive our estimates for the thermodynamic quantities E_0 and H_{298} by adding to these electronic energies ZPVE and the sum of ZPVE and ($H_{298} - E_0$), respectively, where the latter are derived from DFT calculations.

Calculations were carried out for acetylene, ethylene, *o*-, *m*-, and *p*-benzyne, phenyl radical, benzene, the ten isomeric DDN's,

TABLE 2: Zero-Point Vibrational Energies, Thermal Contributions, and Relative State Energies (kcal/mol) for Didehydronaphthalenes[a]

	for given didehydronaphthalene									
	1,2	1,3	1,4	1,5	1,6	1,7	1,8	2,3	2,6	2,7
					Zero-Point Energy[a]					
singlet	74.7	73.8	73.2	73.4	72.7	73.0	73.2	74.6	72.7	72.9
triplet	74.3	74.1	74.3	74.2	74.0	74.1	74.1	73.9	73.9	73.9
					$H_{298} - E_0$[a]					
singlet	5.1	5.1	5.2	5.1	5.3	5.2	5.2	5.1	5.2	5.1
triplet	5.0	5.0	5.0	5.0	5.0	5.0	5.0	5.1	5.0	5.0
					Relative E_0 (CASPT2)[b]					
singlet	0.0[c]	10.8	21.5	19.4	24.8	24.4	25.5	2.1	24.0	23.0
triplet	32.2	28.1	27.1	27.3	25.6	26.0	26.4	30.5	25.8	25.9
					Relative E_0 (DFT)[d]					
singlet	0.0[e]	8.6	28.0	25.4	50.8	42.5	36.9	2.0	47.1	36.8
triplet	33.2	28.3	27.2	27.2	25.4	25.8	26.4	31.5	25.7	26.0

[a] BPW91/cc-pVDZ level. [b] CASPT2(12,12)/cc-pVDZ + BPW91/cc-pVDZ ZPVE. [c] Absolute energy (including ZPVE), −383.249 68 h. [d] BPW91/cc-pVDZ + BPW91/cc-pVDZ ZPVE. [e] Absolute energy (including ZPVE), −384.421 65 h.

TABLE 3: Zero-Point Vibrational Energies, Thermal Contributions, Electronic Energies, and 298 K Heats of Formation for Acetylene, Ethylene, Naphthalene, and Naphthyl Radicals[a]

	acetylene	ethylene	naphthalene	α-naphthyl	β-naphthyl
ZPVE[b]	16.5	31.1	90.1	82.2	82.0
$H_{298} - E_0$[b]	2.4	2.5	5.0	5.0	5.0
E(CASPT2)[c]	−77.082 37	−78.318 53	−384.676 51	−384.001 48	−384.001 64
E(DFT)[b]	−77.319 98	−77.574 57	−385.865 90	−385.182 58	−385.182 41
$\Delta H_{f,298}$	54.35 ± 0.19[d]	12.52 ± 0.12[d]	35.99 ± 0.10[e]	97.4 ± 1.0[f]	97.4 ± 1.0[f]

[a] Electronic energies in hartrees; all other data in kilocalories per mole. [b] BPW91/cc-pVDZ level. [c] See Table 1 for active spaces. [d] Reference 77. [e] Reference 60. [f] See text.

the 1- and 2-naphthyl radicals, and naphthalene. For the benzynes and naphthalynes, separate calculations were carried out for both the lowest energy singlet and triplet states. Table 1 indicates the point group symmetry and active space employed for each of these molecules. S−T splittings and heats of formation are estimated for the DDN's as described in detail in the next section.

Isotropic ^{1}H hyperfine coupling constants in the naphthyl radicals are calculated as[56]

$$a_H = (8\pi/3)gg_H\beta\beta_H\rho(H) \quad (1)$$

where g is the electronic g factor, β is the Bohr magneton, g_H and β_H are the corresponding values for ^{1}H, and ρ(H) is the Fermi contact integral which measures the unpaired spin density at the hydrogen nucleus. The Fermi contact integral is evaluated from

$$\rho(H) = \sum_{\mu\nu} \mathbf{P}^{\alpha-\beta}_{\mu\nu} \phi_\mu(R_H)\, \phi_\nu(R_H) \quad (2)$$

where $\mathbf{P}^{\alpha-\beta}$ is the BPW91/cc-pVDZ one-electron spin density matrix, the summation runs over basis functions ϕ, and evaluation of the overlap between basis functions ϕ_μ and ϕ_ν is only at the hydrogen nuclear position, R_H.

All CAS and DFT calculations were carried out with the MOLCAS[57] and Gaussian 94[58] electronic structure program suites, respectively.

Results

Structures, energies, and selected spectroscopic and thermochemical quantities were computed for the ten isomeric DDN's and related molecules using the CASPT2 and BPW91 methods in conjunction with the cc-pVDZ basis set. The active spaces used for the CAS calculations included the full π-space for each molecule and, for each of the radicals and biradicals, the nonbonding σ orbital(s). The numbers of electrons and orbitals comprising the active spaces are specified in Table 1. Values of the CC bond distances and CCC bond angles obtained by both procedures are summarized in Tables S1−S3 of the Supporting Information for the singlet naphthalynes, triplet naphthalynes, and naphthyl radicals, respectively. The atom numbering scheme is indicated as follows:

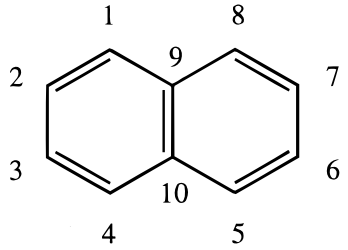

Geometric information obtained at the same levels of theory for *o*-, *m*-, and *p*-benzyne, benzene, phenyl radical, acetylene, and ethylene has been made available in previous work.[45]

Zero-point energy and 298 K thermal contributions to the enthalpy were computed for each molecule from the unscaled vibrational frequencies determined at the BPW91/cc-pVDZ level and are listed in Tables 2−4. These were used in conjunction with the CASPT2 and DFT total energies to derive 0 K energies, E_0, for each naphthalyne singlet and triplet state. These are listed in Table 2 relative to the singlet state of the 1,2-isomer (the global minimum over all isomers and states). The absolute energies for the singlet states of 1,2-naphthalyne, acetylene, ethylene, and for the 1- and 2-naphthyl radicals are also given in Tables 2 and 3. Table 4 lists the DFT zero-point energies, thermal corrections, and CASPT2 total energies for *o*-, *m*- and *p*-benzynes. Also listed are the CASPT2 values of the singlet−triplet splittings, ΔE_{ST}, given by E_0(singlet) − E_0(triplet), as

TABLE 4: Zero-Point Vibrational Energies, Thermal Contributions, Electronic Energies, Singlet−Triplet Splittings, and 298 K Heats of Formation for *o*-, *m*-, and *p*-Benzyne, Phenyl Radical, and Benzene[a]

	o-benzyne	*m*-benzyne	*p*-benzyne	phenyl radical	benzene
			ZPVE[b]		
singlet	45.8	44.7	44.1	53.3	61.4
triplet	45.4	45.2	45.3		
			$H_{298} - E_0$[b]		
singlet	3.5	3.7	3.6	3.4	3.4
triplet	3.4	3.4	3.4		
			E(CASPT2)[c]		
singlet	−230.195 45	−230.179 43	−230.160 91	−230.829 98	−230.504 70
triplet	−230.146 32	−230.151 43	−230.153 50		
			S−T Splitting		
calc[d]	−30.4	−18.0	−5.8		
expt[e]	−37.5 ± 0.3	−21.1 + 0.3	−3.8 + 0.5		
			Singlet $\Delta H_{f,298}$		
calc[f]	106.6	121.6	138.1		
expt	106.6 ± 3.0[g]	121.9 ± 3.1[g]	137.8 ± 2.9[g] 138.0 ± 1.0[h]	81.2 ± 0.6[i]	19.7 ± 0.2[j]

[a] Electronic energies in hartrees; all other data in kilocalories per mole. [b] BPW91/cc-pVDZ level. [c] See Table 1 for active spaces. [d] E_0(singlet) − E_0(triplet). [e] Reference 51. [f] See text for discussion of isodesmic reactions used. [g] Reference 48. [h] Reference 50. [i] Reference 49. [j] Reference 77.

TABLE 5: S−T Splittings (kcal/mol), Singlet Biradical Character Ratios, Triplet SOMO Energies (h) and Energy Gaps (kcal/mol), and Corresponding Doublet hfs Values (G) for Benzynes and Didehydronaphthalenes

	for given benzyne			for given didehydronaphthalene									
	ortho	*meta*	*para*	1,2	1,3	1,4	1,5	1,6	1,7	1,8	2,3	2,6	2,7
S−T gap, CASPT2[a]	−30.4	−18.0	−5.8	−32.2	−17.2	−5.6	−7.8	−0.9	−1.6	−0.9	−28.4	−1.8	−2.9
S−T gap, corrected[b]				−41.1	−20.2	−3.8	−5.8	0.7	−0.3	0.8	−34.8	−0.2	−1.2
C_S^2/C_A^2[c]	12.4	5.2	0.6	13.3	5.1	0.6	0.5	1.0	1.2	0.8	11.4	1.0	1.3
SOMO energies/gaps[d]													
$-E$(S)	0.137	0.128	0.089	0.140	0.129	0.090	0.084	0.099	0.103	0.095	0.136	0.097	0.091
$-E$(A)	0.078	0.076	0.106	0.077	0.078	0.108	0.117	0.100	0.096	0.106	0.081	0.099	0.107
E(S) − E(A)[e]	−36.8	−32.2	10.8	−39.4	−32.2	11.0	20.1	0.5	−4.6	6.5	−35.0	1.2	10.4
^{1}H hfs[f]	15.2	5.9	2.1	17.0	5.6	2.2	3.2	−0.2	0.4	−0.3	13.7	0.3	0.8

[a] CASPT2(8,8) and CASPT2(12,12)/cc-pVDZ for benzynes and didehydronaphthalenes, respectively. [b] Corrected S−T splittings as obtained according to ref 52. [c] CAS(8,8) and CAS(12,12)/cc-pVDZ for benzynes and didehydronaphthalenes, respectively. [d] ROHF/cc-pVDZ. [e] A negative value indicates S below A; values may not agree with direct computation from the above two rows because of rounding. [f] Isotropic hfs calculated at the BPW91/cc-pVDZ level for the hydrogen in 1- or 2-naphthyl radical that would be removed to produce the corresponding biradical.

well as the experimental values determined by negative ion photoelectron spectroscopy.[51]

In seeking patterns in the electronic structures of the DDN's that might reveal the nature of the through-bond coupling between the dehydro centers, HIH examined the symmetries and energy splittings of the two valence orbitals (SOMOs) defined by extended Hückel calculations for each isomer.[24] These molecular orbitals can be designated symmetric (S) or antisymmetric (A), depending upon the relative phases of the two component σ orbitals, i.e., S for the in-phase combination ($\sigma_1 + \sigma_2$) and A for the out-of-phase combination ($\sigma_1 - \sigma_2$). Table 5 gives the absolute energies, symmetries, and energy splittings of these two orbitals, as derived in the present study from ROHF/cc-pVDZ calculations on the triplet state of each naphthalyne at its DFT-optimized geometry. For comparison, the analogous data are provided for *o*-, *m*-, and *p*-benzyne. Also listed in Table 5 for each *singlet* naphthalyne are the ratios C_S^2/C_A^2, where C_S and C_A are the normalized CI coefficients obtained in the CAS calculations for the dominant electron configuration involving double occupation of either the S or A orbital, respectively. A "pure" biradical may be defined as having the two configurations equally populated, and hence $C_S^2/C_A^2 = 1.0$, while systems with significant covalent interaction between the formally unpaired electrons have ratios that are substantially greater than 1.0 (for S below A) or less than 1.0 (for A below S). Also included in Table 5 are the DFT-computed ^{1}H hyperfine coupling constants for corresponding aryl radicals, where the given coupling is for the hydrogen atom that would need to be removed in order to generate the particular naphthalyne listed (in some cases, this number is an average of two possibilities, e.g., for 1,2-naphthalyne it is the average of the hfs for proton 2 of the 1-naphthyl radical and proton 1 of the 2-naphthyl radical; because of the very similar geometries of the two radicals, however, the two values never differ by more than 0.2 G).[52] All three quantities, the coefficient ratios, the SOMO gaps, and the hyperfine splittings, provide some measure of the degree of interaction between the two spins in the aryne and, as such, might be expected to correlate well with S−T splittings, as discussed further in the next section.

Finally, a useful perspective on the relative thermodynamic stabilities of the DDN's derives from consideration of the enthalpy changes for the isodesmic hydrogen-transfer reactions from naphthalene to a naphthalyne biradical to give a pair of 1- and/or 2-naphthyl monoradicals, eq 3. Analogous models

$$C_{10}H_8 + C_{10}H_6 \rightarrow 2C_{10}H_7 \qquad \Delta H_{298} = \text{BSE} \qquad (3)$$

were used in previous theoretical studies of the benzynes,[28,45] α,*n*-didehydrotoluenes,[59] and pyridynes.[29] The enthalpy changes associated with these isodesmic reactions are termed the *biradical stabilization energies* (BSE), as they provide a direct indication of the stabilization (BSE > 0) or destablization (BSE

TABLE 6: Heats of Formation at 298 K for Singlet and Triplet Didehydronaphthalenes Predicted from Isodesmic Reaction Analysis and the Valence Promotion Energy (VPE) Model (kcal/mol)

		for given didehydronaphthalene									
		1,2	1,3	1,4	1,5	1,6	1,7	1,8	2,3	2,6	2,7
						CASPT2					
singlet	BSE or $\Delta H(4)$[a]	−44.3[b]	14.8, −55.2[b]	4.3	6.4	0.8	1.2	0.3	−46.4[b]	−1.4	2.4
	$\Delta H_{f,298}$	122.1	138.5[c]	154.5	152.4	158.1	157.7	158.5	124.2	157.4	156.4
	$\Delta H_{f,298}$, VPE[d]	117.7	138.6	155.0	153.0	159.5	158.5	159.6	124.0	158.6	157.6
triplet	BSE	−6.4	−2.3	−1.1	−1.3	0.1	−0.2	−0.4	−5.0	−0.2	−0.3
	$\Delta H_{f,298}$	165.2	161.1	159.9	160.1	158.8	159.1	159.2	163.8	159.0	159.1
						DFT					
singlet	BSE or $\Delta H(4)$[a]	−43.7[b]	16.7, −52.3[b]						-45.7[b]		
	$\Delta H_{f,298}$	121.5	136.1[c]						123.5		
triplet	BSE	−7.8	−2.9	−1.8	−1.7	0.1	−0.4	−0.9	−6.1	−0.3	−0.5
	$\Delta H_{f,298}$	166.6	161.7	160.6	160.5	158.8	159.2	159.8	165.0	159.1	159.3

[a] All values are BSE (from $\Delta H(3)$) unless otherwise specified. [b] $\Delta H(4)$. [c] Average from use of $\Delta H(3)$ and $\Delta H(4)$. [d] Heat of formation obtained by subtracting corrected S−T splitting (Table 5) from additivity estimate for $\Delta H_{f,298}(C_{10}H_6) = 158.8$ kcal/mol.

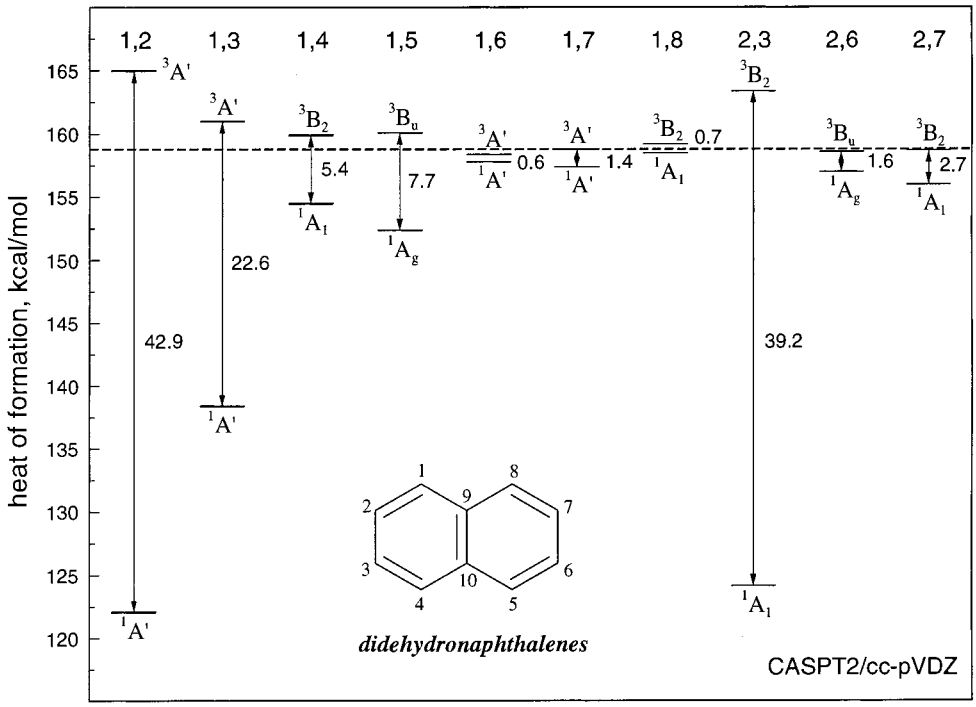

Figure 1. Calculated 298 K heats of formation for singlet and triplet states of the naphthalynes derived from CASPT2/cc-pVDZ enthalpy changes for isodesmic reactions 3 and 4. The dashed line indicates the simple additivity estimate for $\Delta H_{f,298}(C_{10}H_6) = 158.8$ kcal/mol, obtained by assuming that the first and second C−H bond strengths of naphthalene are the same.

< 0) involved when two radical sites are present in the same molecule. BSE values were computed at the CASPT2 and DFT levels for the singlet and triplet states of each naphthalyne isomer from the 298 K enthalpies in Tables 2 and 3 and are listed in Table 6.

BSE values can be used to predict absolute heats of formation for biradicals if the heat of formation of the reference molecule and monoradical(s) are known experimentally. In the present case, naphthalene has an accurately known heat of formation,[60] $\Delta H_{f,298} = 35.99 \pm 0.10$ kcal/mol, but its CH bond strengths have not been measured. However, CASPT2 and DFT calculations indicate that the 1- and 2-CH bond strengths of naphthalene are both the same, to within 0.1 kcal/mol, as that of benzene,[49,61] $\Delta H_{298}(C_6H_5-H) = 113.5 \pm 0.5$ kcal/mol. Therefore, when computing the heats of formation of DDN's with eq 3, we used a value for $\Delta H_{f,298}(C_{10}H_7)$ derived from the experimental heat of formation of naphthalene and an assumed CH bond enthalpy of 113.5 kcal/mol, i.e., $\Delta H_{f,298}(C_{10}H_7) = 97.4$ kcal/mol (Table 3). The predicted heats of formation for the singlet and triplet states of each naphthalyne obtained in this way are listed in Table 6. For the singlet states of 1,2- and 2,3-DDN, the two "cycloalkyne-like" isomers with the least biradical character, the heats of formation were computed with a different isodesmic equation involving double H-atom transfer to acetylene, eq 4.

$$C_2H_4 + C_{10}H_6 \rightarrow C_{10}H_8 + C_2H_2 \qquad (4)$$

For 1,2-biradical singlets this alternative approach provides a far better balance between the correlation energies of the products and reactants than does BSE eq 3—a requirement for accurate thermochemical predictions that we demonstrated in our recent study of the benzynes.[45] For 1,3-naphthalyne, which has intermediate biradical character, the reported heat of formation is the average of the values derived from eqs 3 and 4. This approach was shown in our previous work to give the most accurate estimate for *m*-benzyne.[45] The heats of formation for the singlet and triplet naphthalynes obtained at the CASPT2 level from the isodesmic reaction analysis described above are shown schematically in Figure 1 along with the resulting enthalpy differences. The dashed line represents the heat of

formation of a hypothetical "non-interacting" DDN biradical, 158.8 kcal/mol, which can be derived from experimental data by assuming that the first and second CH bond energies of naphthalene are the same; i.e., BSE = 0 in eq 3.

Discussion

In the following we explore the geometric, electronic, and energetic consequences of interaction between the two radical sites in the DDN's. Through-bond and through-space effects are characterized with the high-level ab initio results and compared with the qualitative predictions made by HIH on the basis of extended Hückel theory. Predictions are made of thermochemical properties (ΔH_f's) and spectroscopic properties (S−T splittings) for the DDN's, and the general lessons these quantities provide about aromatic (σ,σ) biradicals are examined.

Geometries. We focus first on the performance of the two theoretical levels. There is very good agreement in general between DFT and CAS for the geometries of doublet and triplet states. Such agreement is expected given the fairly simple wave functions of these states, which are dominated by a single determinant. For the singlets, DFT shows certain systematic differences with CAS, including shorter bonds between radical centers and adjacent carbons and wider bond angles at the radical centers. Careful comparisons for the six isomeric pyridynes[29] and *p*-benzyne[46] have shown that DFT geometries are in general to be slightly preferred to CAS geometries as judged by well-correlated single-point calculations at other levels of theory (e.g., CCSD(T)). The quality of the DFT geometries for *m*-benzyne[62] and *p*-benzyne[46] critically improves when broken-spin-symmetry calculations are performed, and it is possible that this would also be true for the DDN's with moderately separated radical centers, although we have not undertaken such calculations here since CCSD(T) calculations adjudicating this issue are impractical on systems of this size.

It should also be noted that certain aryne deformations can show very flat potentials. For instance, at the CCSD(T)/cc-pVDZ level the energy of singlet 3,5-pyridyne changes by less than 0.03 kcal/mol over a 0.4 Å change in the separation between the two dehydro positions![29] A similar situation seems to exist with 1,3-naphthalyne. DFT predicts a very short distance of 1.614 Å between the two dehydro positions and very large (9,1,2) and (2,3,4) bond angles, i.e., a nearly bicyclic structure, while CAS predicts a structure not much distorted from the standard naphthalene framework. In the absence of much more rigorous calculations, it is difficult to say which structure is more accurate for 1,3-DDN (and given the expected flat nature of the potential surface, it is not obvious such calculations would be especially interesting). In the case of related *m*-benzyne, photoelectron spectroscopy is consistent with a biradical geometry, not a bicyclic geometry,[51] but in this case BPW91 does not predict a bicyclic structure (although RHF theory does).[45,62]

Given the sensitivities of the singlet geometries to theoretical level, it is more profitable to focus on qualitative aspects of the DDN geometries that are identifiable for *both* levels of theory rather than attempting to interpret differences. One interesting feature that is true for both the CAS and DFT structures is that the bond alternation observed in naphthalene itself, which is predicted from standard resonance theory by consideration of how many resonance structures have a double bond between two connected carbons compared to having a single bond, is maintained in the various DDN's. Thus, the 1,2-bond is shorter than the 2,3-bond in *every* structure except singlet 2,3-DDN (where the 2,3-bond formally has triple bond character rather than aromatic character). This bond alternation impacts the S−T splittings, as discussed further below. We note as well that when a DDN has its two radical centers one in each ring, there is rather little deviation of the geometry from that of naphthalene itself.

Coupling between Radical Centers. One of the key contributions of HIH was to explain the energetic ordering of and the magnitude of the energetic separation between the S and A combinations of the two σ nonbonding orbitals for various locations and coplanar orientations in an extended π system.[24] The primary motivation for this work was to predict biradical reactivity for cases that would be governed by orbital symmetry constraints. In addition, one might legitimately expect the S−T splitting to be large if there is a significant energetic separation between the two nonbonding orbitals. HIH did not evaluate this with their extended Hückel calculations, since they could not distinguish between spin states energetically, but we will further explore the idea below.

The points of HIH most relevant to the DDN's are also relevant to the didehydrobenzenes. These have been discussed in additional detail since that time,[28,63,64] so we summarize the points here only briefly. First, when the two dehydropositions are adjacent to one another, there is a strong through-space overlap having π character (i.e., the species is cycloalkyne-like) that leads to a large separation with S below A. Second, when the relationship is 1,3 within the same ring (i.e., *meta* in the benzyne case), there continues to be significant through-space interaction between the back lobes of the nonbonding orbitals so that S is again well below A. Although they did not comment on it, the calculations of HIH indicate that interaction between the back lobes of the two nonbonding orbitals is strongly enhanced by a mixing with the intervening C−H σ* (cf. Table V of ref 24). This observation may well explain the particularly flat nature of the potential surface in 1,3-arynes: decreasing the "bond" distance between the dehydrocenters improves the direct overlap of the nonbonding orbitals but raises the energy of the C−H σ* by compressing the bond angle at the 2-position (and thus decreases its ability to mix with the S combination of the nonbonding orbitals). This suggests that substitution at the 2-position may significantly affect the structures and S−T splittings of 1,3-arynes—such an observation is consistent with results obtained for 2,6-pyridyne[29] and 2,3-didehydrophenyl anion,[65] where in each case it is now an intervening *occupied* orbital (the lone pair) that most significantly perturbs the 1,3-aryne.

HIH also pointed out the A below S nature of the nonbonding hybrids for collinear 1,4-biradicals (e.g., *p*-benzyne) that arises from a through σ-bond coupling mediated by the intervening parallel 2,3-σ* orbital (and the symmetrically related 5,6-σ* for *p*-benzyne or 9,10-σ* for 1,4-DDN). Table 5 indicates that all of the features of HIH's analysis at the Hückel level are equally true at the ROHF level, and indeed the quantitative agreement between the S/A orbital separations in the benzynes and separations in the analogous naphthalynes is quite good. Finally, HIH predicted the S/A ordering for the biradical geometries found in 1,5-, 1,8-, and 2,7-naphthalyne (orderings which agree with the ROHF levels in Table 5) but did not discuss the details of the orbital hybridizations for these cases. They did note that, for 1,8- and 2,7-naphthalynes, it was not obvious whether stabilizing two-electron interactions with intervening virtual orbitals were perturbatively stronger or weaker than destabilizing four-electron interactions with intervening filled orbitals.

We see no need to amplify extensively on this analysis, other than to note the following: (1) The A below S separation for

1,5-DDN is much larger than for 1,4-DDN, consistent with the observation that there is some through-space antibonding interaction between the 1- and the 4-positions for the A molecular orbital in 1,4-DDN that is absent in 1,5-DDN since the orbitals are no longer collinear (HIH actually calculated the magnitude of the antibonding through-space interaction for *p*-benzyne and found it to be only slightly less than the through-space *bonding* interaction in *m*-benzyne). This larger S/A separation in the 1,5-case is consistent with the greater S−T gap in this isomer (vide infra). (2) The S/A separation in 2,7-DDN is surprisingly large, given the significant separation between the two didehydro centers. However, strong nuclear/nuclear and nuclear/electron coupling in such "W-like" configurations (sometimes called "zigzag coupling") is a well-known phenomenon in NMR[66] and EPR[67] spectroscopies, respectively, that is conceptually analogous and indicates that the W-framework permits good overlap between atomic orbitals along the path that contributes to the hybrid MO. (3) While the S/A orderings and separations provide insight into the electronic structure of the biradicals, they do not *necessarily* provide any information about the S−T splittings. That is, the one-electron orbital energy from the ROHF procedure for the triplet state is not necessarily a good predictor of the energy splitting between the singlet and triplet states, the latter being a many-electron property. This is especially problematic if the two states have spatially different MO's, which may be expected when the formally nonbonding orbitals are coupled so that spin−spin interactions influence the orbital shapes. We now proceed to a more in-depth analysis of S−T splittings, which is the ultimate measure of coupling between the two radical centers.

Singlet−Triplet Splittings. Table 5 collects the calculated S−T splittings for the DDN's along with a number of other data that might be expected to correlate well with spin-state energy separations. Values for ΔE_{ST} obtained directly from the CASPT2 energy differences are listed along with the "corrected" S−T splittings derived by scaling the CASPT2 values as described in our previous report[52] (vide infra). S−T gaps from DFT are not provided (although they can be determined from the data in Table 2) since DFT energies are unreliable for many of the singlets as discussed more fully elsewhere.[52] Nevertheless, it is worth noting that, for 1,2- and 2,3-DDN, the DFT gaps agree with the CASPT2 gaps to within 1 kcal/mol. This is interesting for the 1,2 case because the two spin states have the same spatial symmetry, namely A′, and there is thus no *formal* expectation that DFT should be capable of predicting this gap (the Kohn−Sham theorem has been proven only for the lowest energy spin state of each irreducible representation of the molecular point group[68])—a further analysis of this point is beyond the scope of this article.

As noted above, correlations between spin-state energy splittings and other data are of interest to the extent they may provide an economical predictive model. In the course of addressing that point, we note a variety of other interesting features of the splittings that merit discussion.

First, the preference for the singlet state in 1,2-DDN is about 2 kcal/mol larger than the corresponding preference in *o*-benzyne, while for 2,3-DDN the preference is about 2 kcal/mol *smaller* than *o*-benzyne. As noted previously by Ford and Biel,[44] this derives from the bond alternation found in all of the naphthalene-derived species—since the 1,2-bond is intrinsically shorter than the 2,3-bond, there is less distortion cost to forming the formal triple bond in the former than the latter, and *o*-benzyne is intermediate between the two. This bond alternation does not impact on the S−T splittings of 1,3- and 1,4-DDN, which are within 1 kcal/mol of the corresponding values for *m*- and *p*-benzyne. Comparison of the corrected S−T splittings with the experimental[51] splittings of *o*-, *m*-, and *p*-benzyne leads to the same conclusions.

Another interesting observation is the larger preference for the singlet state exhibited by 1,5-DDN compared to 1,4-DDN. As discussed above, we assign this to the elimination of through-space antibonding interactions in the A HOMO of 1,5-DDN that are present in the corresponding A HOMO of 1,4-DDN. A different example of the importance of relative orientation of the nonbonding orbitals and the pathway connecting them is offered by comparison of the S−T splittings for 1,6- and 2,7-DDN, both of which have four σ bonds between the dehydro positions. The former has degenerate singlet and triplet states within the expected accuracy of the calculations, while the latter has a 2 kcal/mol larger preference for the singlet state, indicating the strength of W-coupling in this configuration as discussed above. Another instance where relative orbital orientation plays an important role is 1,8-DDN. Although 1,3-DDN and 1,8-DDN both have only two σ bonds separating the two dehydro centers, the former shows a strong singlet preference while the latter has essentially degenerate singlet and triplet states. The near degeneracy in the 1,8-system might not be expected, given the 6.5 kcal/mol energy gap between the S and A nonbonding MO's in this isomer. This illustrates the limitations of using the S/A separation as a simple tool for predicting S−T splittings.

To quantify this point, we may consider the quality of the relationship between S/A orbital separation and S−T splitting. First, we note that the correlation between S−T splitting and the distance separating the two dehydrocenters is low (R^2 = 0.703 for the 13 data points in Table 5);[52] if through-space interactions dominated the spin−spin coupling, one would expect this correlation to be higher. The relationship between S−T splitting and the S/A separation, on the other hand, has a correlation coefficient R^2 of 0.909. Thus, the S/A separation contains some information about through-bond coupling, but it is limited by being specific to the triplet and the ROHF procedure. An alternative indicator of the coupling between the two dehydro centers is the C_S^2/C_A^2 ratio in the biradical singlets, where C_S and C_A are defined in Results. This increases the correlation coefficient to 0.941 but is still not very satisfying, since one point of having a simple predictive model is to avoid having to do costly CAS calculations on the multiconfigurational singlets.

The correlation between the S−T splitting and proton hyperfine coupling constants in the appropriate monoradicals (i.e., the coupling to the proton at the position that would create the particular biradical upon its removal in the monoradical) is still more quantitative, with a correlation coefficient R^2 of 0.970. This correlation was used[52] in conjunction with the experimental S−T splittings for the benzynes[51] to derive the corrected splittings for the DDNs listed in Table 5. The strong correlation between proton hyperfine couplings and S−T splittings is intuitive insofar as each is a measure of the degree to which a spin (in one case nuclear, in the other electronic) at one position interacts with a spin at another position. Interestingly, the hfs calculations predict *negative* spin density for the 6- and 8-positions of 1-naphthyl radical and for the 5-position of 2-naphthyl radical. Removal of a hydrogen from these positions leads to either the 1,6- or 1,8-diradicals, and these are the two cases where the ΔE_{ST} scaling procedure leads to predictions of triplet ground states.[52] We examine this point more closely.

Population analysis of the spin densities in the 1- and 2-naphthyl radicals reveals the π systems to be spin-polarized in the manner shown as follows:

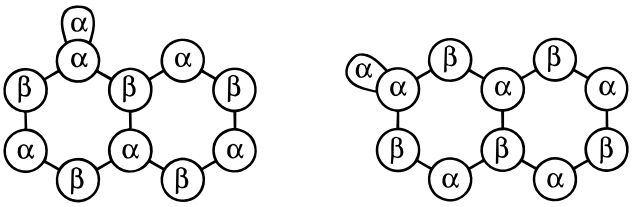

This is a natural consequence of the reduced electron repulsion energy that results from high-spin coupling of the σ and π electrons at the dehydrocarbons,[69] and the usual alternation of the π spin polarization between adjacent sites.[70−73] If one now considers removal of a hydrogen atom from the monoradicals to create a second unpaired electron, then it is evident from the above diagrams that, in order to maintain high-spin coupling between the σ and π electrons at the new dehydrocarbon, net triplet states are favored for dehydrogenation at positions 3, 6, and 8 of the 1-naphthyl radical and positions 4, 5, and 7 of the 2-naphthyl radical.[59] The corrected S−T splittings do lead to the prediction that 1,6-DDN (which is also 2,5-DDN if numbered according to the original radical site) and 1,8-DDN are ground-state triplets.

The remaining cases, however, are influenced by other factors that are operative at shorter range than π polarization. Thus, 1,3-DDN has short-range through-space and through-σ-bond couplings that overwhelm polarization effects in the π system, and 2,7 exhibits the medium-range W-coupling in the σ system that also appears to outweigh π polarization effects.

To summarize, in analyzing the interactions between the formally unpaired electrons that lead to the computed S−T splittings, there is a three-way interplay of through-space interactions that dominate at very short range, through σ-bond interactions that extend over a greater range, particularly for certain optimal frameworks and nonbonding orbital orientations, and, lastly through π-bond (or aromatic) interactions that extend out to the longest range. Spin delocalization in monoradicals can provide an accurate measure of the importance of these effects in biradicals and hence provides a cheap method for estimating S−T splittings in the latter.

Thermochemistry. Table 4 compares the experimentally determined heats of formation for *o*-, *m*-, and *p*-benzyne with the calculated values obtained at the CASPT2/cc-pVDZ level in conjunction with isodesmic reactions 5 and 6 and the known

$$C_6H_6 + C_6H_4 \rightarrow 2C_6H_5 \quad (5)$$

$$C_2H_4 + C_6H_4 \rightarrow C_6H_6 + C_2H_2 \quad (6)$$

heats of formation of benzene, phenyl radical, ethylene, and acetylene. Excellent agreement with experiment is found for the singlet heats of formation when eq 5 is used for *p*-benzyne, eq 6 for *o*-benzyne, and the average of the two for *m*-benzyne. As discussed in detail previously,[45] this protocol takes into account the differing extent of covalent interaction between the dehydrocarbons in the three benzynes. An analogous procedure was employed to derive heats of formation for the naphthalynes using the data listed in Tables 2 and 3 in conjunction with eqs 3 and 4. These results are listed in Table 6. DFT singlet energies are unreliable for most naphthalynes, so the heats of formation obtained from DFT for those species are not included in Table 6. However, there is good agreement between the CASPT2 and DFT results for the 1,2-, 1,3-, and 2,3-DDN singlets, as well as for all the triplets.

Experimental heats of formation are available for a few of the singlet naphthalynes. Linnert and Riveros[43] assigned a heat of formation of 122 ± 6 kcal/mol to both 1,2- and 2,3-DDN based on the occurrence and nonoccurrence of halide elimination from reactions of halonaphthalenes with various anions carried out in an ion cyclotron resonance spectrometer. Roth et al.[37] measured activation energies for both the Bergman cyclization of 1,2-diethynylbenzene and the retro-Bergman rearrangement of 1,4-DDN from which a 298 K heat of formation for the biradical of 152.9 ± 1.4 kcal/mol was derived. The CASPT2 calculations are comfortably within the experimental error limits for 1,2- and 2,3-DDN, while for the 1,4-isomer the computed value is 0.2 kcal/mol outside the error limits. The computed heats of formation for the other isomers are expected to be of comparable accuracy, i.e., within 2−3 kcal/mol of the true values.

The BSE analysis for 1,6- and 1,8-DDN leads to heats of formation for the singlet states that are slightly lower than those of the triplet states, while the corrected S−T splittings for these biradicals (Table 5) suggest triplet ground states. The differences are very small, in any case, such that both spin states are likely to be thermally populated in any experiments involving these biradicals. The same may be said for 1,7-, 2,6-, and 2,7-DDN, since the S−T splittings are also quite small (≤1 kcal/mol).

We can use the computed heats of formation for the singlet and triplet naphthalynes along with our best estimates for the S−T splittings (Table 5) to assess the performance of the valence promotion energy (VPE) model for singlet biradical thermochemistry which has been advanced by Chen and co-workers.[74,75] The VPE model equates the hypothetical "non-interacting" DDN biradical with its triplet state, which allows one to estimate the heat of formation for the singlet ground state by simply, subtracting the S−T gap from the bond-strength additivity value for $\Delta H_f(C_{10}H_6)$ of 158.8 kcal/mol (vide supra). These estimates are listed in Table 6. There is good agreement between the heats of formation derived from isodesmic reaction analysis and the VPE model for all but 1,2-DDN, where the VPE model predicts a heat of formation that is 4.4 kcal/mol lower. Moreover, the differences in the heats of formation for the singlet and triplet states (Figure 1) are larger than the corrected S−T splittings (Table 5) by about 2 kcal/mol for all but 2,3-DDN, where the difference is 4.4 kcal/mol greater than the predicted S−T gap. For biradicals with strong through-space interactions, one might expect the VPE model to give estimates for singlet biradical heats of formation that are too low because in these systems the triplet state will be a poor representation of the "non-interacting" biradical if it is strongly destabilized by overlap repulsion.[28,76] However, the experimental thermochemical data for the benzynes[51] indicate that these effects are small (<1 kcal/mol for *o*-benzyne). It seems likely that the overlap repulsion effects are overestimated by the CASPT2 calculations, which leads to heats of formation for 1,2-, 2,3- and, to a lesser extent, for 1,3-, 1,4-, and 1,5-DDN that are systematically too high.

Conclusions

CASPT2 and DFT calculations provide semiquantitative predictions of structural and energetic properties for the DDN's. When appropriate isodesmic equations are employed, thermochemical estimates in good agreement with known heats of formation for three naphthalyne isomers are obtained.

Spin−spin interaction in DDN biradicals takes place via three distinct mechanisms that vary in magnitude and range. Of the three, polarization of the π system extends to the longest range and favors singlet coupling of the spins when an odd number of σ-bonds separates the two radical centers and triplet coupling when an even number of σ-bonds intervene. This effect is fairly small in magnitude, however, and at shorter range coupling of the formally nonbonding σ orbitals through naphthalene framework σ orbitals leads to orbital mixing that can reduce the biradical character of the naphthalyne.

In certain instances, the symmetric or antisymmetric mixing of the two nonbonding orbitals that leads to the most stable hybrid MO can be readily predicted because communication between the two is primarily mediated by a single intervening type of orbital, e.g., $\sigma^*_{C(2)-C(3)}$ and parallel $\sigma^*_{C(9)-C(10)}$ make the dominant contributions to the coupling between the nonbonding orbitals in 1,4-DDN, and hence the phase of the lower energy hybrid is, like those two σ^* orbitals, antisymmetric across the vertical plane bisecting the 1,4-axis. In other cases, however, the relative orientation of the nonbonding orbitals does not allow for a particularly strong through-σ-bond coupling to be realized (or, more accurately, the coupling in the singlet is smaller than other favorable energetic effects present in the triplet)—such a situation is manifest for 1,8-DDN.

Finally, through-space interactions (i.e., simple overlap) dominate when the nonbonding orbitals are adjacent to one another, as in 1,2- and 2,3-DDN, or are *meta*-related in the same ring, as in 1,3-DDN. Such species, are found to have a strong preference for singlet ground states.

The extent of spin−spin interaction in the DDN biradicals is also indicated by their calculated thermochemical properties. The predicted heats of formation based on isodesmic reaction analysis indicate a 37 kcal/mol range of relative stabilities for the singlets, with the 1,2- and 2,3-DDN isomers being lowest in energy and the 1,6- and 1,8- being the highest in energy. The relative stabilities of the singlet DDNs generally parallel the magnitudes of the S−T splittings, in accord with the valence promotion energy model. Insofar as aromatic substituents might be used to adjust the energies and spatial extent of critical framework orbitals used in the nonbonding MOs of the DDNs, it seems reasonable to speculate that an even larger range of relative stabilities can be accessed within aryne systems of this size, and, hence, tuning of biradical reactivities in didehydronaphthalenes with potential pharmaceutical utility seems a viable option.

Acknowledgment. We are grateful for high-performance vector and parallel computing resources made available by the Minnesota Supercomputer Institute and the University of Minnesota−IBM Shared Research Project, respectively. This work was supported in part by the National Science Foundation and the Alfred P. Sloan Foundation.

Supporting Information Available: Tables (S1−S3) of bond lengths and valence bond angles for the naphthalynes, naphthalene, and the naphthyl radicals (6 pages). Ordering information is given on any current masthead page.

References and Notes

(1) *Enediyne Antibiotics as Antitumor Agents;* Borders, D. B., Doyle, T. W., Eds.; Dekker: New York, 1995.
(2) Nicolaou, K. C.; Dai, W.-M. *Angew. Chem.* **1991**, *103*, 1453.
(3) Poon, R.; Beerman, T. A.; Goldberg, I. H. *Biochemistry* **1977**, *16*, 486.
(4) Myers, A. G.; Cohen, S. B.; Kwon, B.-M. *J. Am. Chem. Soc.* **1994**, *116*, 1670.
(5) Myers, A. G.; Kuo, E. Y.; Finney, N. S. *J. Am. Chem. Soc.* **1989**, *111*, 8057.
(6) Myers, A. G.; Parrish, C. A. *Bioconjugate Chem.* **1996**, *7*, 322.
(7) Goldberg, I. H.; Kappen, L. S.; Xu, Y.-j.; Stassinopoulos, A.; Zeng, X.; Xi, Z.; Yang, C. F. In *DNA and RNA Cleavers and Chemotherapy of Cancer and Viral Diseases;* Meunier, B., Ed.; Kluwer: Amsterdam, 1996; p 1.
(8) Jones, R. R.; Bergman, R. G. *J. Am. Chem. Soc.* **1972**, *94*, 660.
(9) Bergman, R. G. *Acc. Chem. Res.* **1973**, *6*, 25.
(10) Wender, P. A.; Zercher, C. K. *J. Am. Chem. Soc.* **1991**, *113*, 2311.
(11) Myers, A. G.; Dragovich, P. S.; Kuo, E. Y. *J. Am. Chem. Soc.* **1992**, *114*, 9369.
(12) Semmelhack, M. F.; Gallagher, J. J.; Minami, T.; Date, T. *J. Am. Chem. Soc.* **1993**, *115*, 11618.
(13) Grissom, J. W.; Calkins, T. L.; Mcmillen, H. A.; Jiang, Y. H. *J. Org. Chem.* **1994**, *59*, 5833.
(14) Elbaum, D.; Nguyen, T. B.; Jorgensen, W. L.; Schreiber, S. L. *Tetrahedron* **1994**, *50*, 1503.
(15) Semmelhack, M. F.; Gallagher, J. J.; Ding, W. D.; Krishnamurthy, G.; Babine, R.; Ellestad, G. A. *J. Org. Chem.* **1994**, *59*, 4357.
(16) Iida, K.-i.; Hirama, M. *J. Am. Chem. Soc.* **1995**, *117*, 8875.
(17) Schmittel, M.; Steffen, J. P.; Bohn, I. *Heterocycl. Commun.* **1997**, *3*, 443.
(18) Lindh, R.; Ryde, U.; Schütz, M. *Theor. Chem. Acc.* **1997**, *97*, 203.
(19) Schreiner, P. R. *J. Chem. Soc., Chem. Commun.* **1998**, 483.
(20) Chen, P. *Angew. Chem.* **1996,** *108*, 1584.
(21) Logan, C. F.; Chen, P. *J. Am. Chem. Soc.* **1996,** *118*, 2113.
(22) Schottelius, M. J.; Chen, P. *J. Am. Chem. Soc.* **1996,** *118*, 4896.
(23) Hoffner, J.; Schottelius, M. J.; Feichtinger, D.; Chen, P. *J. Am. Chem. Soc.* **1998**, *120*, 376.
(24) Hoffmann, R.; Imamura, A.; Hehre, W. J. *J. Am. Chem. Soc.* **1968**, *90*, 1499.
(25) Hoffmann, R. *Acc. Chem. Res.* **1970**, *4*, 1.
(26) Gleiter, R. *Angew. Chem., Int. Ed. Engl.* **1974**, *13*, 696.
(27) Paddon-Row, M. N. *Acc. Chem. Res.* **1992**, *15*, 245.
(28) Wierschke, S. G.; Nash, J. J.; Squires, R. R. *J. Am. Chem. Soc.* **1993**, *115*, 11958.
(29) Cramer, C. J.; Debbert, S. *Chem. Phys. Lett.* **1998**, *287*, 320.
(30) Bunnett, J. G.; Brotherton, T. K. *J. Am. Chem. Soc.* **1956**, *78*, 155.
(31) Roberts, J. D.; Semenow, D. A.; Simmons, H. E.; Carlsmith, L. A. *J. Am. Chem. Soc.* **1956**, *78*, 601.
(32) Darby, N.; Kim, C. U.; Salaün, J. A.; Shelton, K. W.; Takada, S.; Masamune, S. *J. Chem. Soc., Chem. Commun.* **1972**, 1516.
(33) Myers, A. G.; Finney, N. S. *J. Am. Chem. Soc.* **1992**, *114*, 10986.
(34) Just, G.; Singh, R. *Tetrahedron Lett.* **1990,** *31*, 185.
(35) Boger, D. L.; Zhou, J. *J. Org. Chem.* **1993**, *58*, 3018.
(36) Semmelhack, M. F.; Neu, T.; Francisco, F. *J. Org. Chem.* **1994,** *59*, 5038.
(37) Roth, W. R.; Hopf, H.; Wasser, T.; Zimmerman, H.; Werner, C. *Liebigs Ann. Chem.* **1996,** 1691.
(38) Bharucha, K. N.; Marsh, R. M.; Minto, R. E.; Bergman, R. G. *J. Am. Chem. Soc.* **1992,** *114*, 3120.
(39) Averdung, J.; Mattay, J. *Tetrahedron Lett.* **1994**, *35*, 6661.
(40) Weimer, H. A.; McFarland, B. J.; Li, S.; Weltner, W. *J. Phys. Chem.* **1995**, *99*, 1824.
(41) Grützmacher, H. F.; Lohmann, J. *Liebigs Ann. Chem.* **1970**, *733*, 88.
(42) Grützmacher, H. F.; Lehmann, W. R. *Liebigs Ann. Chem.* **1975**, 2023.
(43) Linnert, H. V.; Riveros, J. M. *Int. J. Mass Spectrom. Ion. Processes* **1994**, *140*, 163.
(44) Ford, G. P.; Biel, E. R. *Tetrahedron Lett.* **1995**, *36*, 3663.
(45) Cramer, C. J.; Nash, J. J.; Squires, R. R. *Chem. Phys. Lett.* **1997**, *277*, 311.
(46) Cramer, C. J. *J. Am. Chem. Soc.* **1998**, *120*, 6261.
(47) Lindh, R.; Schütz, M. *Chem. Phys. Lett.* **1996**, *258*, 409.
(48) Wenthold, P.; Squires, R. R. *J. Am. Chem. Soc.* **1994**, *116*, 6401.
(49) Davico, G. E.; Bierbaum, V. M.; DePuy, C. H.; Ellison, G. B.; Squires, R. R. *J. Am. Chem. Soc.* **1995**, *117*, 2590.
(50) Roth, W. R.; Hopf, H.; Horn, C. *Chem. Ber.* **1994**, *127*, 1765.
(51) Wenthold, P. G.; Squires, R. R.; Lineberger, W. C. *J. Alm. Chem. Soc.*, in press.
(52) Cramer, C. J.; Squires, R. R. *J. Phys. Chem. A* **1997**, *101*, 9191.
(53) Dunning, T. H. *J. Chem. Phys.* **1989**, *90*, 1007.
(54) Becke, A. D. *Phys. Rev. A* **1988**, *38*, 3098.
(55) Perdew, J. P.; Burke, K.; Wang, Y. *Phys. Rev. B* **1996**, *54*, 6533.
(56) Lim, M. H.; Worthington, S. E.; Dulles, F. J.; Cramer, C. J. In *Density-Functional Methods in Chemistry;* Laird, B. B., Ross, R. B., Ziegler, T., Eds.; American Chemical Society: Washington, DC, 1996; p 402.
(57) Andersson, K.; Blomberg, M. R. A.; Fülscher, M. P.; Karlström, G.; Kelli, V.; Lindh, R.; Malmqvist, P.-Å.; Noga, J.; Olsen, J.; Roos, B. O.; Sadlej, A. J.; Siegbahn, P. E. M.; Urban, M.; Widmark, P.-O. *MOLCAS-3;* University of Lund: Lund, Sweden, 1994.

(58) Frisch, M. J.; Trucks, G. W.; Schlegel, H. B.; Gill, P. M. W.; Johnson, B. G.; Robb, M. A.; Cheeseman, J. R.; Keith, T.; Petersson, G. A.; Montgomery, J. A.; Raghavachari, K.; Al-Laham, M. A.; Zakrzewski, V. G.; Ortiz, J. V.; Foresman, J. B.; Cioslowski, J.; Stefanov, B. B.; Nanayakkara, A.; Challacombe, M.; Peng, C. Y.; Ayala, P. Y.; Chen, W.; Wong, M. W.; Andres, J. L.; Replogle, E. S.; Gomperts, R.; Martin, R. L.; Fox, D. J.; Binkley, J. S.; Defrees, D. J.; Baker, J.; Stewart, J. J. P.; Head-Gordon, M.; Gonzalez, C.; Pople, J. A. *Gaussian 94 Rev. D.1;* Gaussian Inc.: Pittsburgh, PA, 1995.

(59) Wenthold, P. G.; Wierschke, S. G.; Nash, J. J.; Squires, R. R. *J. Am. Chem. Soc.* **1994**, *116*, 7378.

(60) Chirico, R. D.; Knipmeyer, S. e.; Nguyen, A.; Steele, W. V. *J. Chem. Thermodyn.* **1993**, *25*, 1461.

(61) Cioslowski, J.; Liu, G.; Martinov, M.; Piskorz, P.; Moncrieff, D. *J. Am. Chem. Soc.* **1996**, *118*, 5261.

(62) Kraka, E.; Cremer, D.; Bucher, G.; Wandel, H.; Sander, W. *Chem. Phys. Lett.* **1997**, *268*, 313.

(63) Nicolaides, A.; Borden, W. T. *J. Am. Chem. Soc.* **1993**, *115*, 11951.

(64) Kraka, E.; Cremer, D. *J. Am. Chem. Soc.* **1994**, *116*, 4929.

(65) Squires, R. R. Unpublished calculations.

(66) Sternhell, S. *Q. Rev. Chem. Soc.* **1969**, *23*, 236.

(67) King, F. W. *Chem. Rev.* **1976**, *76*, 157.

(68) Gunnarsson, O.; Lundqvist, B. I. *Phys. Rev. B* **1976**, *13*, 4274.

(69) Salem, L. *Electrons in Chemical Reactions;* Wiley: New York, 1982; Chapter 7.

(70) McConnell, H. M. *J. Chem. Phys.* **1963**, *39*, 1910.

(71) Iwamura, H. *Adv. Phys. Org. Chem.* **1990**, *26*, 179.

(72) Kollmar, C.; Kahn, O. *Acc. Chem. Res.* **1993**, *26*, 259.

(73) Yoshizawa, K.; Hoffmann, R. *J. Am. Chem. Soc.* **1995**, *117*, 6921.

(74) Zhang, X.; Chen, P. J. *J. Am. Chem. Soc.* **1992**, *114*, 3147.

(75) Blush, J. A.; Clauberg, H.; Kohn, D. W.; Minsek, D. W.; Zhang, X.; Chen, P. *Acc. Chem. Res.* **1992,** *25*, 385.

(76) Jorgensen, W. L.; Borden, W. T. *J. Am. Chem. Soc.* **1973**, *95*, 6649.

(77) Gurvich, L. V.; Veyts, I. V.; Alcock, C. B. *Thermodynamic Properties of Individual Substances*, 4th ed.; Hemisphere: New York, 1991; Vol. 2, Parts 1 and 2.